ELSEVIER

Earth and Planetary Science Letters 183 (2000) 107–120

EPSL

www.elsevier.com/locate/epsl

# Regional geochemistry and continental heat flow: implications for the origin of the South Australian heat flow anomaly

Narelle Neumann *, Mike Sandiford [1], John Foden

*Department of Geology and Geophysics, Adelaide University, Adelaide, S.A. 5005, Australia*

Received 15 May 2000; received in revised form 5 September 2000; accepted 19 September 2000

**Abstract**

Existing measurements from South Australia define a broad (> 250 km wide) zone of anomalously high surface heat flow (92 ± 10 mW m$^{-2}$). This zone is centred on the western margin of the Adelaide Fold Belt (Neoproterozoic to early Phanerozoic cover floored by Palaeoproterozoic to Mesoproterozoic basement), where it borders the eastern Gawler Craton and Stuart Shelf (Palaeoproterozoic–Mesoproterozoic). To the west, in the western Gawler Craton (Archaean to Palaeoproterozoic), heat flow averages ∼54 mW m$^{-2}$ while to the east in the Willyama Inliers (Palaeoproterozoic) heat flow averages ∼75 mW m$^{-2}$. We use a regional geochemical dataset comprising > 2500 analyses to show that the anomalous heat flow zone correlates with exceptional surface heat production values, mainly hosted in Palaeoproterozoic to Mesoproterozoic granites. The median heat production of Precambrian 'basement' rocks increases from < 3 μW m$^{-3}$ west of the anomalous zone to ∼6 μW m$^{-3}$ within the anomalous zone. In the highest known part of the heat flow anomaly, Mesoproterozoic gneisses and granites of the Mount Painter Province in the northern Adelaide Fold Belt yield an area-integrated mean heat production of 9.9 μW m$^{-3}$. These data suggest that the anomalous heat flow reflects an unusual enrichment in U and Th in this part of the Proterozoic crust, with the total complement of these elements some 2–3 times greater than would be expected for Proterozoic crust on the basis of the global heat flow database. This extraordinary enrichment has played an important role in modulating the thermal regime of the crust in this region, and particularly its response to tectonic activity. 

*Keywords:* heat flow; regional patterns; heat sources; South Australia; Proterozoic; granites

## 1. Introduction

The thermal structure of continental interiors is fundamental to their long-term tectonic and geochemical evolution. Our understanding of thermal regimes within the continental crust has been greatly influenced by surface heat flow measurements. These measurements are particularly important because they yield information concerning the thermal structure of the lithosphere and constrain the vertical distribution of heat sources [1–3]. Further, heat flow data provide a unique insight into the geochemistry of the crust because they constrain the depth integrated abundance of

* Corresponding author. Tel.: +61-8-8303-4868; Fax: +61-8-8303-4347; E-mail: narelle.neumann@adelaide.edu.au

[1] Present address: School of Earth Sciences, University of Melbourne, Parkville, Vic. 3010, Australia.

0012-821X/00/$ – see front matter 
PII: S0012-821X(00)00268-5

heat-producing elements [4,5]. In the recent past, considerable effort has been expended towards understanding global heat flow averages, and the source distributions that contribute to them (e.g. [3,6–8]). While such global averages are undoubtedly important, their significance should be evaluated with regard to the following points. Firstly, the so-called global heat flow dataset is strongly biased by measurements made in North America, Europe and southern Africa, with the heat flow field from other continental regions virtually unknown. Secondly, given that many important geological processes are temperature dependent, the natural spatial variation in thermal parameters is of greater relevance than global averages. In this regard, regions of elevated heat flow are fundamental to our understanding of the thermal structure of the continental crust.

This paper concerns itself with a region of elevated heat flow in South Australia. Existing heat flow measurements in this region suggest either anomalous mantle activity or that radiogenic crustal sources contribute more than twice what would be expected on the basis of global heat flow averages. In this region, crustal growth occurred mainly from the Palaeoproterozoic through to the early Mesoproterozoic [9]. Heat flow measurements are often of poor quality or display broad scatter, and as with all such measurements there is a need to evaluate their plausibility. A primary purpose of this paper is to determine the validity of these heat flow values in light of inferences about mantle thermal regimes and surface heat production parameters derived from regional geochemical and geophysical datasets. These data suggest that the anomalous heat flow reflects extraordinary concentrations of heat-producing elements in the crust. In Section 6, we briefly explore the origin and implications of this exceptionally enriched crust.

## 2. Some preliminary remarks concerning global heat flow

Surface heat flow is a measure of the combined heat flow from the convective mantle, radiogenic heat from the decay of U, Th and K within the lithosphere and transient perturbations associated with tectonic, magmatic, hydrologic and/or climatic activity. Over 10 000 global continental heat flow measurements [7] have been used to constrain the chemical and thermal structure of the lithosphere. However, it should be stressed that 90% of these measurements are from three continents; Europe, North America and Africa. In comparison, the heat flow field of South America, Australia and Asia is relatively poorly known, while Antarctica is virtually unknown. Note also that almost all heat flow measurements within Africa come from either the Archaean provinces of southern Africa or the East African rift, with the heat flow field of the great majority of the continent outside these provinces only very poorly known. An important question, therefore, concerns just how representative the existing heat flow dataset is.

Although the global heat flow dataset suggests marked spatial and temporal variations, existing measurements have been used to constrain the crustal contribution to the surface heat flow average. Using a reduced heat flow value of 27 mW $m^{-2}$, McLennan and Taylor [5] proposed that 'the crustal radiogenic crustal component of continental heat flow must lie within the range of 18–48 mW $m^{-2}$, and almost certainly lies in the range 21–34 mW $m^{-2}$'. This range correlates well with crustal heat flow contributions of 20 to $>$44 mW $m^{-2}$ calculated using geochemical and seismic data from Archaean and Proterozoic crustal sections together with average surface heat flow values [3,10–14].

A major focus of previous heat flow studies has been the relationship between surface heat flow and tectonic age (Fig. 1). An inverse relationship is suggested by the available data which increase from 41 mW $m^{-2}$ for the Archaean, 51–54 mW $m^{-2}$ for Proterozoic areas, 61 mW $m^{-2}$ for the Late Palaeozoic and 72 mW $m^{-2}$ for Cenozoic to Mesozoic terranes [2,15,16]. High values within young tectonothermal terranes are interpreted to reflect transient thermal perturbations associated with tectonic/magmatic activity, whereas variations between Archaean and Proterozoic terranes reflect different crustal heat production distributions or mantle heat flow contributions [15].

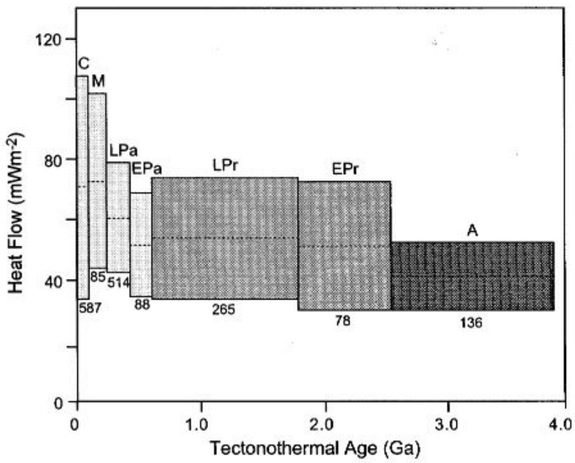


Fig. 1. Global surface heat flow averaged in groups according to the age of the last major tectonothermal event, from [15,16]. Age key: A–Archaean, EPr–Early Proterozoic, LPr–Late Proterozoic, EPa–Early Palaeozoic, LPa–Late Palaeozoic, M–Mesozoic, C–Cenozoic. The dashed line represents the mean heat flow value for that group and the boxes indicate the age ranges for the data and standard deviations of the means. The number of data in each group is listed below that box. Dark grey shading for Archaean, mid-grey for Proterozoic and light-grey for Phanerozoic data.

Previous investigations have also noted that there are significant variations in heat flow according to their proximity to Archaean–Proterozoic boundaries, with values of $\sim$40 mW m$^{-2}$ for Proterozoic crust within 100–400 km of Archaean cratons increasing to 54–58 mW m$^{-2}$ in Proterozoic regions greater than 400 km from cratonic regions [8]. Although differences in crustal heat production may contribute to the spatial variation in heat flow, the observed signature has been primarily attributed to differences in lithospheric thickness, with heat diverted around thick cold Archaean roots into the surrounding younger terrains [8,17].

While the global heat flow average for continental lithosphere has been used as the basis for studies of the thermal evolution in many Precambrian terranes, heat flow values within Proterozoic Australia are significantly higher than the global average for terranes of comparable, or younger age. On the basis of 90 measurements within Australia, Sass and Lachenbruch [18] identified three heat flow provinces: the primarily Archaean Western Shield Province (ages $>$2500 Myr), the mainly Proterozoic Central Shield Province (600–2000 Myr) and the Palaeozoic Eastern Province (Fig. 2). While the average heat flow of 39 mW m$^{-2}$ within the Western Shield Province is consistent with other shield areas of similar age, the Central Shield Province records significantly elevated heat flow, with 32 determinations providing a mean of 83$\pm$20 mW m$^{-2}$. Heat flow in the Eastern Province is also elevated, with 38 measurements producing an average of 72 mW m$^{-2}$. Sass and Lachenbruch [18] proposed a reduced heat flow contribution of 27 mW m$^{-2}$ throughout all provinces, with differences in surface heat flow reflecting lateral variations in crustal heat production in the two western zones and additional thermal effects of magmatic and tectonic activity in the Eastern Province. Such an interpretation requires that within the Central Shield Province, internal heat sources contribute $>$50 mW m$^{-2}$

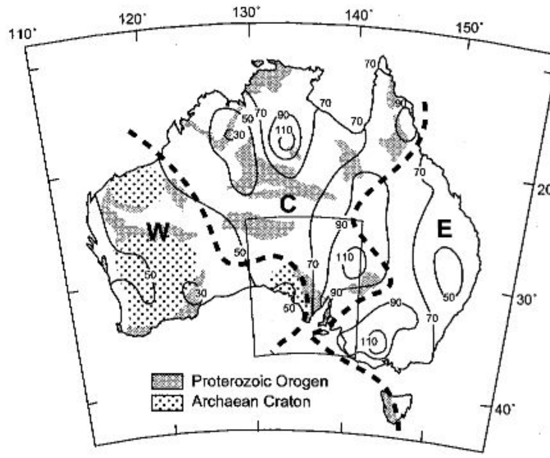


Fig. 2. Surface heat flow map of Australia (after [18]) showing the main outcrops of Precambrian crystalline basement. The three provinces, W, C and E, represent adaptations of Sass and Lachenbruch's [18] Western Shield, Central Shield and Eastern Province, respectively. W is characterised by heat flows mostly less than 50 mW m$^{-2}$ and represents the part of the continent formed principally in the Archaean. C, with heat flows typically in the range 50–90 mW m$^{-2}$, comprises portions of the continent where the principal continental growth occurred in the Proterozoic. E, with variable heat flow character, represents terranes accreted to the Australian continent during the Phanerozoic. Note that the boundary between W and C occurs in the middle of the Gawler Craton in South Australia (see Figs. 3 and 4).

to the surface heat flow. This implies that a significant proportion of the Australian continent lies near, or beyond, the upper limit of the range of crustal heat production parameters suggested by the global heat flow dataset (e.g. [5]). If this assertion can be corroborated, it would imply that the natural variation in heat flow within continents should be revisited, with any inferences about global heat flow averages cognisant of the potential bias introduced by the geography of the available data. South Australia has the most detailed heat flow record within the Central Shield Province and therefore provides an ideal setting to assess the validity of the elevated heat flow measurements. In order to evaluate the South Australian heat flow record, we will first outline the geological framework of this region.

## 3. Geological setting

South Australia is dominated by two Archaean–Proterozoic cratonic terranes separated by the Adelaide Fold Belt (Fig. 3). Unless otherwise stated, all geochronological data are from Drexel et al. [19] and Daly et al. [20]. The western region of South Australia comprises the Gawler Craton, a stable crystalline basement terrane composed of Archaean to Mesoproterozoic magmatic and metasedimentary rocks. The northern and western boundaries of the Gawler Craton are covered by the sedimentary Neoproterozoic Officer Basin and the Cenozoic Eucla Basin, respectively. The northeastern part of the Craton is covered by a thin veneer of Neoproterozoic sediments of the Stuart Shelf, and the eastern extent is defined by the Torrens Hinge Zone (Fig. 3). The Gawler Craton has been divided into numerous subdomains based on tectonic, chemical and isotopic constraints [19]. Western subdomains are dominated by Archaean to Early Proterozoic crust-forming events including the Sleaford and Mulgathing Complexes. In contrast, the eastern Gawler Craton is dominated by younger crust-forming events, with Late Palaeoproterozoic magmatism in the Cleve, Lincoln and Moonta subdomains including the ∼1850 Ma bimodal Lincoln Batholith and ∼1700 Ma granites and minor mafics. The final voluminous magmatic event of the eastern and northern Gawler Craton is the anorogenic ∼1600–1575 Ma Hiltaba Suite and associated Gawler Range Volcanics (Fig. 3).

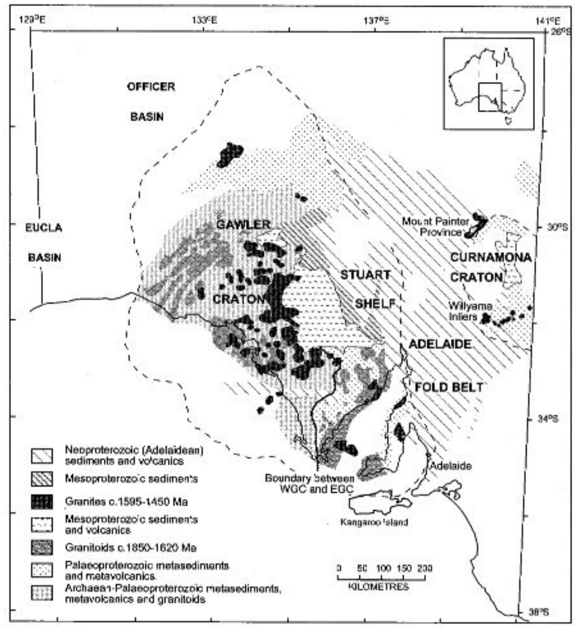


Fig. 3. Summary of main Precambrian elements of South Australian geology (adapted from Drexel et al. [19]). Dashed lines represent the inferred boundaries of the Gawler Craton and Curnamona Craton.

The Adelaide Fold Belt contacts the eastern Gawler Craton and Stuart Shelf along the Torrens Hinge Zone, which marks the western limit of Neoproterozoic sedimentation in the Adelaide Geosyncline (see Fig. 3). Late Palaeoproterozoic–Mesoproterozoic basement inliers within the fold belt include the northern Mount Painter Province; a Palaeoproterozoic metasedimentary sequence intruded by 1575–1555 Ma granites and volcanics. In the northeast, the Willyama Inliers (which include the Olary and Broken Hill Blocks) expose Palaeoproterozoic sedimentary and volcanic units intruded by granites at ∼1720–1700 Ma and ∼1590 Ma [21]. These basement terranes are unconformably overlain by a thick Neoproterozoic to Early Cambrian cover sequence of clastics, carbonates and minor volcanics deposited within an aborted, intracratonic rift forming the Adelaide Geosyncline. Both basement and cover were deformed and partly metamorphosed during the Delamerian Orogeny (~500 Ma) to form the Adelaide Fold Belt. The Curnamona Craton comprises eastern–central South Australia and is bounded by the northern Adelaide Fold Belt to the west and the Willyama Inliers to the south (Fig. 3). Although poorly exposed, the Curnamona Craton appears to be of similar age to the eastern Gawler Craton and Willyama Inliers.

## 4. Surface heat flow in South Australia

Existing heat flow values from 22 different locations within South Australia (Table 1) increase from west to east, with a distinct rise in values evident between the western and eastern Gawler Craton (Fig. 4). The zone of elevated heat flow, which we term the South Australian heat flow anomaly (SAHFA), overlaps the boundary between the eastern Gawler Craton and the Adelaide Fold Belt, including the Stuart Shelf (Fig. 3). Heat flow measurements at the Olympic Dam Cu–U–Au-REE deposit on the Stuart Shelf provide the most detailed heat flow dataset within the SAHFA. Measurements from seven locations excluding the Olympic Dam deposit yield a heat flow average of 73 mW m$^{-2}$, while the heat flow recorded at the orebody is 125 mW m$^{-2}$ [23].

Table 1
South Australian heat flow data

| Province | Site | Lat (°S) | Long (°E) | $n$ | $Q$ (mW m$^{-2}$) | $H$ (μW m$^{-3}$) | Source |
|---|---|---|---|---|---|---|---|
| WGC | Maralinga | 30.17 | 131.60 | | 54 | | [22] |
| | Tarcoola | 30.62 | 134.50 | 20 | 49 | 2.7 | [22] |
| | Wudinna | 32.98 | 135.55 | 17 | 58 | 4.9 | [22] |
| EGC | Iron Knob | 32.72 | 137.13 | 6 | 109 | 7.5 | [22] |
| | Whyalla | 33.17 | 137.50 | 2 | 91 | 8.4 | [22] |
| | Kadina | 33.97 | 137.75 | | 101 | | [22] |
| | Bute | 33.87 | 138.02 | | 88 | | [22] |
| | Bute | 33.93 | 137.97 | | 87 | | [22] |
| | Wokurna | 33.72 | 138.12 | | 91 | | [22] |
| SS | Olympic Dam RD21 | | | | 125 | | [23] |
| | Andamooka BLD1 | | | | 67 | | [23] |
| | WRD2[a] | | | | 78 | | [23] |
| | IDD1[a] | | | | 62 | | [23] |
| | ACD3[a] | | | | 101 | | [23] |
| | SGD2[a] | | | | 84 | | [23] |
| | HHD1[a] | | | | 86 | | [23] |
| | BD2[a] | | | | 50 | | [23] |
| MPP | Parabarana Hill | 29.98 | 139.72 | 4 | 126 | 7.9 | [22] |
| AFB | Ediacara | 30.60 | 138.12 | | 96 | | [22] |
| | Mount McTagga | 30.45 | 139.30 | | 101 | | [22] |
| | Carrieton | 32.55 | 138.48 | | 92 | | [22] |
| | Stockyard | 34.77 | 138.80 | | 88 | | [22] |
| | Kanmantoo | 35.08 | 139.25 | | 88 | | [22] |
| | Bendigo St | 33.20 | 139.47 | 12 | 64 | 3.8 | [22] |
| WI | Mootooroo | 32.25 | 140.93 | 11 | 68 | 3.1 | [22] |
| | Radium Hill | 32.50 | 140.50 | 4 | 75 | 3.8 | [24] |
| | Broken Hill | 31.95 | 141.47 | 56 | 80 | 4.6 | [25] |
| SESA | Mount Gambier | 37.75 | 140.86 | | 92 | | [22] |

$n$ = number of heat flow determinations. $Q$ = surface heat flow. $H$ = surface heat production. Provinces: WGC = western Gawler Craton, EGC = eastern Gawler Craton, SS = Stuart Shelf, MPP = Mount Painter Province, AFB = Adelaide Fold Belt, WI = Willyama Inliers, SESA = south–east South Australia.
[a]Heat flow measurements located within 3 km of Olympic Dam RD21.

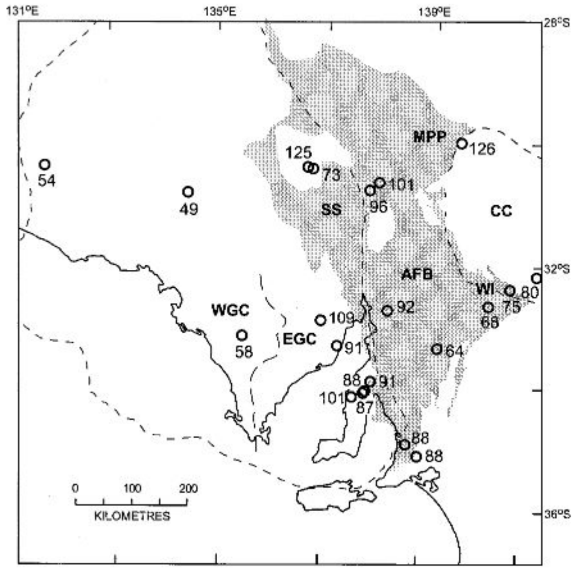


Fig. 4. Distribution of South Australian heat flow records, with the main crustal element boundaries. See Fig. 3 for geological detail. Shaded area represents outcrop extent of Neoproterozoic sedimentation. Dashed lines as for Fig. 3. Province abbreviations: WGC = western Gawler Craton, EGC = eastern Gawler Craton, SS = Stuart Shelf, MPP = Mount Painter Province, AFB = Adelaide Fold Belt, WI = Willyama Inliers, CC = Curnamona Craton. Heat flow data from [22–25].

Accompanying U–Th assay data suggest that $\sim 30$ mW m$^{-2}$ of the additional heat flow is generated within the orebody at depths less than 1 km, with the excess heat flow presumably originating at greater depths [23,26]. The maximum heat flow recorded within the SAHFA is 126 mW m$^{-2}$ from Parabarana Hill in the Mount Painter Province although, as outlined later, the thermal regime at this locality may be significantly modified by recent tectonism and hydrothermal activity. The eastern Adelaide Fold Belt, in the vicinity of the Willyama Inliers, is characterised by somewhat lower, but still elevated heat flows of 68–81 mW m$^{-2}$ (Fig. 4).

Regression of the South Australian heat flow data for which basement heat production measurements are reported yields a poorly constrained slope (or characteristic length-scale, $h_r$) of 9.7 km, and intercept (or reduced heat flow, $q_r$) of 29.5 mW m$^{-2}$. The poor fit is probably due to a combination of factors, including the incorporation of measurements from different heat flow provinces (see below). The mean and standard deviation of all 22 heat flow records from South Australia is $86 \pm 20$ mW m$^{-2}$. In order to further define the character of the SAHFA, we will focus on heat flow measurements within this region. Exclusion of the western Gawler Craton ($n = 3$, $54 \pm 5$ mW m$^{-2}$) increases the SAHFA to $91 \pm 17$ mW m$^{-2}$ (Fig. 5). By further excluding the somewhat lower values from the Willyama Inliers and eastern Adelaide Fold Belt ($n = 4$, $72 \pm 7$ mW m$^{-2}$) and the anomalously high measurements from Mount Painter, the Olympic Dam deposit and Mount Gambier, the remaining 11 records define a mean heat flow of $92 \pm 10$ mW m$^{-2}$ (Fig. 5). This is our best estimate for the regional character of the SAHFA.

The extent of the SAHFA is not precisely constrained from the available data (Figs. 2 and 4). It clearly extends from Adelaide in the south some 600 km north to the Mount Painter Province. North of Mount Painter it appears to merge with a broad heat flow anomaly extending almost all the way across the continent (Fig. 2), although the density of data in the interior of the continent is too low to critically evaluate this. The most westerly record within the SAHFA is at Iron Knob, although the anomaly may well extend as far westwards as 136°E, which represents the ap-

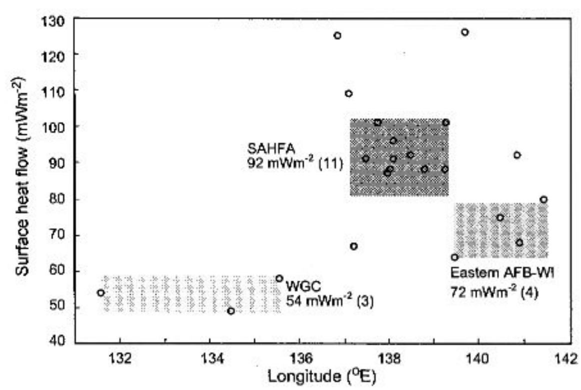


Fig. 5. Surface heat flow values as a function of longitude across South Australia. The three boxes denote the main regional heat flow groups (province abbreviations as for Fig. 4), with the average heat flow value for each region and number of measurements in brackets. Heat flow data from [22–25].

proximate longitude of the boundary between the eastern and western Gawler Craton (Fig. 4). Although the eastern boundary is relatively poorly defined, the anomaly extends as far eastwards as the Mount Painter Province at $\sim$140°E giving a minimum width of 250 km. The available data suggest that the Willyama Inliers are characterised by somewhat elevated heat flows, and thus could also be included in the SAHFA, in which case the anomaly is over 500 km across.

Heat flow values in the SAHFA are extraordinary in the context of averages reported for other Proterozoic terranes. For example, the Grenville province of North America is probably the best characterised Late Proterozoic province, with 30 heat flow determinations providing an average of $41 \pm 11$ mW m$^{-2}$ [27] which makes it one of the 'coldest' known continental regions. In view of the elevated heat flow signature in South Australia, it is appropriate to assess whether these values are a true reflection of the regional lithospheric thermal budget. In principle, the anomalous heat flow could be the result of a number of factors including recent tectonism or magmatism, hydrologic processes, abnormal mantle heat flow and/or exceptional concentrations of heat-producing elements in the crust. In this section, we discuss the evidence pertaining to these possibilities.

### 4.1. Recent tectonism

The SAHFA overlaps a region of mild neotectonic activity which has resulted in the formation of the Flinders Ranges. It is broadly coincident with, and represents a reactivation of the Adelaide Fold Belt, which contrasts the adjacent Gawler Craton and Stuart Shelf, where there is no evidence of significant fault-related displacement since the Mesoproterozoic. The age of the initial uplift of the modern Flinders Ranges is still debated and may be as old as Eocene, or as recent as late Pliocene [28]. The coincidence of the uplands with a belt of active low-level, seismicity supports the notion that tectonism is ongoing, as do widespread Pleistocene fanglomerate aprons in the footwall to steep reverse faults that typically bound the uplands. While transient thermal anomalies associated with denudation of this upland system cannot explain the elevated heat flow in the eastern Gawler Craton (Fig. 4), they may be responsible for some anomalies within the Flinders Ranges. In particular, the very high heat flow (126 mW m$^{-2}$) from the Mount Painter region may be influenced by such recent tectonism, as this measurement is located on the bounding escarpment of the upland system.

### 4.2. Magmatic activity

Southeastern Australia contains a well defined, recent volcanic province that includes the very south–east corner of South Australia. [29]. While this magmatic province is also associated with elevated heat flow (e.g. Mount Gambier [22]), the province is more than 400 km from the nearest measurement used to define the SAHFA and up to 1000 km from its north–westerly limit. This magmatism can therefore be dismissed as a significant contributor to the SAHFA. An older period of magmatism is represented by the Jurassic Wisanger Basalt at Kangaroo Island [30], however, this is again well south of any measurement used to define the SAHFA and is sufficiently old that any associated transient thermal anomalies would have decayed by now.

### 4.3. Hydrologic activity

The northeastern interior of South Australia contains Mesozoic sedimentary basins associated with the vast aquifer system of the Great Artesian Basin. Thermal gradients in these basins often exceed 50°C km$^{-1}$ and are locally as high as 70°C km$^{-1}$ [31]. These basins extend as far south as the northern limits of the Stuart Shelf and the northern Adelaide Fold Belt. However, none of the heat flow measurements that define the SAHFA is from areas where these aquifers are known to exist. Moreover, the majority of the measurements are within crystalline basement, where there is no independent evidence for significant hydrologic activity. The only documented example of hydrothermal activity within the heat flow anomaly is from Parabarana Hill, where the nearby active Paralana Hot Springs may significantly modify the measured heat flow.

### *4.4. Abnormal mantle heat flow*

A number of observations and inferences bear on the thermal regime of the upper mantle beneath the SAHFA. Firstly, the absence of significant tectonism and magmatic activity in the region since the early Phanerozoic suggests that the mantle lithosphere is in no way thermally anomalous. By analogy with provinces of similar age elsewhere in the world, we might expect relatively thick lithosphere at least beneath the eastern Gawler Craton, where the last tectonic activity of any significance was in the Mesoproterozoic. This notion is corroborated by estimates of upper mantle seismic velocity [32] which show that the region is underlain by material of relatively fast seismic velocity at depths of 100–200 km. This contrasts with the more easterly parts of Australia, which are characterised by significantly slower upper mantle velocities. The boundary between these various mantle domains coincides with the eastern limit of Proterozoic crust, some 500 km east of the SAHFA.

The relatively fast upper mantle velocities beneath the SAHFA suggest relatively cool upper mantle temperatures, and can be used to constrain the contributions of mantle and crustal heat sources to the observed surface heat flow. Here we outline some simple calculations that allow estimation of the contributions assuming that, to account for the fast seismic velocities, the uppermost mantle must be no hotter than $\sim 500$°C. We begin by noting that for a given surface heat flow ($q_s$) and conductivity ($k$), Moho temperatures depend on both the heat flow at depth ($q_m$), and the way in which the crustal contribution to heat flow, $q_c$ (where $q_c = q_s - q_m$) is distributed within the crust as represented by the length-scale, $h$ [33]. For the thermal arguments developed below this length parameter is given by the mean depth defined as:

$$h = \frac{1}{q_c}\int_0^{z_c} (H(z)z)\mathrm{d}z$$

where $H$ is the heat production rate and $z_c$ is the base of the crust, beneath which there is assumed to be negligible heat production. Sandiford and McLaren [33] show that with $h$ defined in this way, the temperature at any depth, $z$, beneath the heat-producing parts of the crust is given by:

$$T(z) = (q_m z + q_c h)/k$$

For any assumed functional heat production distribution, the parameter $h$ can be easily related to parameter $h_r$ inferred from regression of surface heat production and heat flow data [33]. For the exponential model of Birch et al. [34] and others, $h = h_r$. For a heat production distribution which consists of a layer of homogeneous heat production of thickness $h_r$, $h = h_r/2$.

We now consider the thermal consequences at upper mantle depths ($\sim 40$ km) of the various combinations of $q_m$, $q_c$ and $h$ consistent with the SAHFA where $q_s$ is $\sim 90$ mW m$^{-2}$. $h$ can be constrained by recognising that the crustal contribution to the surface heat flow $q_c = H_s h$, where $H_s$ is the characteristic surface heat production, and assuming the functional form of the heat production distribution. Regression of the surface heat flow–heat production data suggests the SAHFA is characterised by $h \sim 10$ km and $q_r \sim 30$ mW m$^{-2}$, with a resulting $q_c$ of 60 mW m$^{-2}$. For these parameters, $T_{40\,\mathrm{km}}$ is estimated to be 600°C for an assumed exponential distribution or 500°C for an assumed homogeneous distribution (Fig. 6). While these calculations are sensitive to the assumed thermal conductivity, about which there is some uncertainty, they suggest that for the relatively fast upper mantle seismic velocities, $q_m$ can be no more than 30 mW m$^{-2}$. If the distribution more closely approximates an exponential distribution than a homogeneous distribution, then $q_m$ must be no more than about 15 mW m$^{-2}$ (Fig. 6). Note that if the elevated heat flow was entirely due to anomalous mantle contributions (i.e. $q_m \sim 60$ mW m$^{-2}$), $T_{40\,\mathrm{km}}$ must exceed 800°C, which would seem to require significantly slower upper mantle velocities than suggested by Zielhuis and van der Hilst [32].

### *4.5. Enrichment in crustal heat production*

The SAHFA forms part of a province that

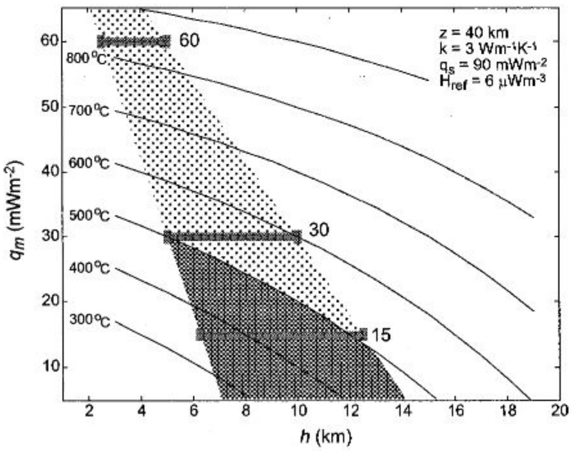


Fig. 6. Illustration of the effect of partitioning of heat flow between mantle and crustal sources on upper mantle temperatures. Figure indicates estimated temperatures at 40 km depth with a surface heat flow of 90 mW m$^{-2}$ and a crustal heat production of 6 μW m$^{-3}$, as suggested by Fig. 7. The heat production distribution, $h$, ranges from the exponential model ($h = h_r$) to the homogeneous model ($h = h_r/2$). Assuming that these heat production distributions bracket the range in $h$ that characterise the continental crust, the shaded area shows the range of Moho temperatures that could apply to the SAHFA. Regression of surface heat production–heat flow data suggests $q_r = 30$ mW m$^{-2}$ and $h = 10$ km. Equating $q_r$ with $q_m$ for these conditions yields Moho temperatures of 500–600°C depending on the distribution. If the surface heat flow is entirely due to anomalous mantle heat contributions (i.e. $q_m = 60$ mW m$^{-2}$ and $q_c = 30$ mW m$^{-2}$), then Moho temperatures would exceed 800°C, while mantle heat flows of 15 mW m$^{-2}$ ($q_c = 75$ mW m$^{-2}$) yield Moho temperatures in the range 360–525°C.

hosts several significant uranium deposits, the most notable being the giant Olympic Dam deposit. Such occurrences suggest that the province may be unusually enriched in heat-producing elements, and it is therefore pertinent to explore the possibility that elevated crustal heat production provides the additional heat flow within the SAHFA. If the anomalous heat flow was entirely of a crustal origin, then these sources would be required to contribute at least 60 mW m$^{-2}$. Assuming a length-scale, $h$, of 10 km then the characteristic surface heat production required to produce the anomaly would be 6 μW m$^{-3}$, which is more than three times higher than the upper crustal heat production average of 1.8 μW m$^{-3}$ [5].

In order to evaluate this possibility, we have compiled all existing geochemical data for Archaean to Mesoproterozoic lithologies from South Australia. Heat production values have been calculated as present day averages from U, Th and $K_2O$ geochemical analyses (data from [35–39]; unpublished data). U, Th and K concentrations were obtained from whole rock powders using a X-ray fluorescence spectrometer. Detection limits for U and Th are 1.5 ppm, with an accuracy of ±5% at 100× detection limit for U and Th and ±0.02% for $K_2O$ wt%. These detection limits and resultant uncertainties are only significant for samples with low U, Th and K concentrations. For instance, for U = 5 ppm, Th = 20 ppm and $K_2O$ = 3.00 wt%, the calculated $H$ is 3.0 μW m$^{-3}$ with an error of ±0.5 μW m$^{-3}$ (17%). The error becomes more insignificant at higher concentrations; for $H = 6$ μW m$^{-3}$ the error is only ±8% assuming standard crustal ratios of U, Th and $K_2O$. For reference, average heat production values for typical lithologies range from 0.1 μW

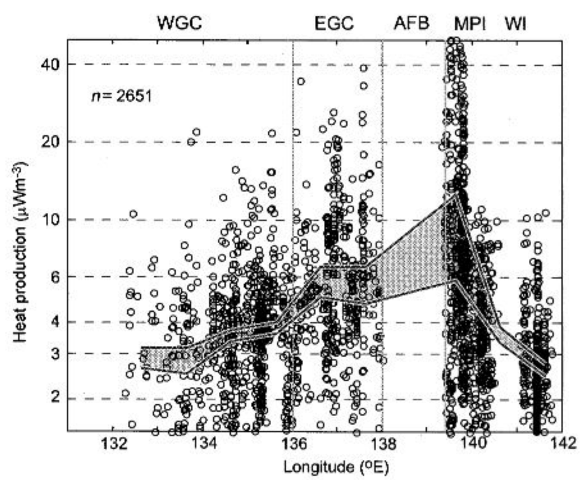


Fig. 7. Surface heat production values from South Australian Precambrian basement terranes plotted as a function of longitude. Heat production values calculated from whole rock geochemical analyses. The upper bound of the shaded region is defined by the binned average of the heat production data, the lower bound by the binned median. Note logarithmic scale for heat production values. The absence of data in the interval 138–139.5°E is due to the fact that in this region the Precambrian basement is covered by the Neoproterozoic sediments of the AFB. Province abbreviations as for Fig. 4. Data from [35–39]; unpublished data.

Table 2
Average U, Th and K concentrations and heat production values for selected units of the SAHFA

| | Lithological groups | $n$ | U (ppm) | Th (ppm) | $K_2O$ (wt%) | Th/U | H ($\mu W\ m^{-3}$) |
|---|---|---|---|---|---|---|---|
| EGC | Hutchison Group | 13 | 7 | 25 | 1.78 | 3.6 | 3.9 |
| | Donington Suite | 40 | 5 | 27 | 4.48 | 5.4 | 3.7 |
| | Myola Volcanics | 3 | 6 | 26 | 5.23 | 4.3 | 4.0 |
| | Moonta Porphyry | 20 | 11 | 39 | 5.02 | 3.5 | 6.2 |
| | McGregor Volcanics | 10 | 9 | 42 | 3.49 | 4.7 | 5.8 |
| | Wandearah Metasiltstone | 13 | 7 | 17 | 3.92 | 2.4 | 3.4 |
| | Middlecamp Granite | 25 | 10 | 61 | 5.16 | 6.1 | 7.6 |
| | Moody Suite | 27 | 10 | 22 | 4.83 | 2.2 | 4.8 |
| | Burkitt Granite | 11 | 37 | 93 | 5.85 | 2.5 | 17.0 |
| | Carappee Granite | 2 | 9 | 46 | 5.38 | 5.1 | 6.1 |
| | Hiltaba Suite-Coulta/Cleve | 15 | 10 | 41 | 5.32 | 4.1 | 6.0 |
| | Hiltaba Suite-Lincoln | 16 | 17 | 85 | 5.47 | 5.0 | 11.1 |
| | Hiltaba Suite-Moonta | 22 | 17 | 61 | 4.47 | 3.6 | 9.4 |
| | Hiltaba Suite-Stuart Shelf | 54 | 14 | 55 | 5.64 | 3.9 | 8.3 |
| MPP | Basal Metasediments | 18 | 14 | 18 | 3.85 | 1.3 | 5.3 |
| | Freeling Heights Quartzite | 3 | 2 | 7 | 1.97 | 3.5 | 1.2 |
| | Mount Neill Granite, Pepegoona Porphyry | 60 | 21 | 74 | 3.57 | 3.5 | 11.3 |
| | Hot Springs Gneiss | 42 | 75 | 288 | 4.17 | 3.8 | 41.0 |
| | Box Bore Granite, microgranites | 30 | 44 | 131 | 6.37 | 3.0 | 21.6 |
| | Yerila Granite | 28 | 116 | 423 | 5.66 | 3.6 | 61.6 |
| | Wattleowie Granite | 27 | 6 | 33 | 5.78 | 5.5 | 4.5 |
| | Terrapinna Granite | 29 | 10 | 58 | 5.24 | 5.8 | 7.2 |
| | Petermorra Volcanics | 7 | 13 | 35 | 6.50 | 2.7 | 6.7 |

$n$ = number of samples used to calculate average concentrations of U, Th and $K_2O$. $H$ = average current heat production. Units divided between the EGC and MPP (abbreviations as for Table 1) and listed in geochronological order. Data from [35–39] and unpublished data.

$m^{-3}$ for tholeiitic basalts and 2.1 $\mu W\ m^{-3}$ for shales, to 2.5 $\mu W\ m^{-3}$ for granites [40,41].

The surface heat production distribution of ~2650 samples as a function of longitude clearly indicates that the SAHFA is characterised by elevated concentrations of heat-producing elements (Fig. 7). There is a distinct rise in median heat production from ~3 $\mu W\ m^{-3}$ in the western Gawler Craton to ~5 $\mu W\ m^{-3}$ for the eastern Gawler Craton. Surface heat production reaches a maximum within the Mount Painter Province where the range is extreme (1–65 $\mu W\ m^{-3}$), the average is ~11 $\mu W\ m^{-3}$ and median is ~6 $\mu W\ m^{-3}$. To the east, heat production decreases to a median value of ~2.5 $\mu W\ m^{-3}$ in the eastern Willyama Inliers.

An obvious query about the treatment of the data using binned averages or means is that no account is taken of the relative volumetric contribution of each of the rock types that comprise the various provinces. For much of South Australia poor outcrop precludes detailed assessment of area-integrated heat production rates. This is particularly true of the Gawler Craton, which is mostly covered by a thin veneer of aeolian sand. In contrast, excellent outcrop in the Mount Painter Province allows for the construction of relatively well constrained heat production maps. Using both airborne radiometric data and whole rock geochemistry, Sandiford et al. [42] were able to show that the area-integrated surface heat production for the province is 9.9 $\mu W\ m^{-3}$. We suggest that the area-integrated heat production for the transect is bracketed by the binned mean and median heat production estimates, with representative upper crustal heat production falling in the region highlighted by shading in Fig. 7.

In order to assess the extent to which the heat

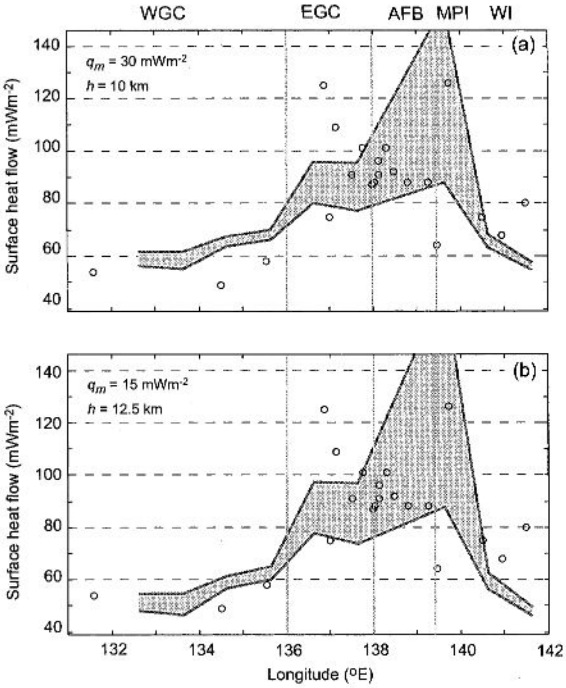


Fig. 8. Surface heat flow measurements plotted as a function of longitude. The shaded area is the calculated surface heat flow obtained by using the binned average (upper bound) and median (lower bound) heat production data assuming in (a) a length-scale $h = 10$ km and mantle heat flow $q_m$ of 30 mW m$^{-2}$, and in (b) a length-scale $h = 12.5$ km and mantle heat flow $q_m$ of 15 mW m$^{-2}$ (see text for discussion). Heat flow data from [22–25].

production distribution may account for the observed heat flow, we have modelled the surface heat flow using the median and mean of the binned heat production data shown in Fig. 7, for two different sets of $h$–$q_m$ parameters. In Fig. 8a, we assume $q_m = 30$ mW m$^{-2}$ and $h = 10$ km, while in Fig. 8b, we assume $q_m = 15$ mW m$^{-2}$ and $h = 12.5$ km. In detail, the median heat production tends to slightly underestimate the heat flow within the SAHFA (by $\sim$5–10 mW m$^{-2}$), slightly overestimate the heat flow in the western Gawler Craton, and greatly underestimate the heat flow in the Willyama Inliers (by up to 25 mW m$^{-2}$) for both sets of distribution parameters. In contrast, the mean heat production data tend to overestimate heat flows in all but the Willyama Inliers. These figures show that for all but the Willyama Inliers there is a first order correlation between observed heat flow and heat production. Within the limits of the approach, this corroborates the notion that the South Australian heat flow field is largely explicable in terms of crustal heat production distributions. While this applies to both the western Gawler Craton and SAHFA, it would appear that no single set of $h$–$q_m$ parameters can account for the heat flow of both regions. In particular, the data seem to suggest that the western Gawler Craton is characterised by a slightly lower value of $q_m$ and/or $h$ than the SAHFA. A lower value of $q_m$ would not be surprising given that the western Gawler Craton is believed to have formed in the Archaean and is therefore somewhat older than the provinces that comprise the SAHFA. In contrast with the western Gawler Craton and SAHFA, heat production values for the Willyama Inliers do not seem to be sufficient to account for the heat flow in this zone.

## 5. Heat production in the SAHFA

Given that the concentration of heat-producing elements in the SAHFA is anomalously high, it is appropriate to identify the source of the elevated heat production distribution. For this purpose, heat production values for the main Proterozoic lithologies in this region have been compiled (Table 2). Calculated heat production values for metasedimentary units within this transect are consistent with accepted lithological means and show little variation across provinces, suggesting that they do not contribute to the SAHFA. In contrast, granitic and volcanic lithologies display a large range in heat production, with many units within the eastern Gawler Craton and especially the Mount Painter Province containing extremely elevated values. Although U and Th concentrations within these granites are extreme, corresponding Th/U values are dominantly 3–5 (Table 2), suggesting that this enrichment is a primary magmatic signature.

The heat production compilation highlights the fact that the region of high heat flow in South Australia coincides with the occurrence of Proterozoic granites and volcanics which contain anomalously high U, Th and K concentrations. This suggests that Proterozoic felsic magmatic events have been important in shaping the vertical distribution of radiogenic elements in the crust. There is also good evidence for an increase in the upper range of heat production values for granites through time from the Archaean to the Mesoproterozoic, with the youngest granites in this region representing the final voluminous magmatic event in the Proterozoic. Within the SAHFA, heat production values for the Late Palaeoproterozoic Donington Suite average $\sim$4 μW $m^{-3}$, increase to 5–8 μW $m^{-3}$ for $\sim$1700 Ma granites and remain high at $\sim$9 μW $m^{-3}$ for Hiltaba granites of the eastern Gawler Craton and Stuart Shelf (Table 2). As described in the Section 4, heat production reaches a maximum at Mount Painter, which also contains the youngest Proterozoic granites in the SAHFA.

Because these heat production anomalies are geochemical phenomena and their source and distribution seem intimately associated with granite formation, the question of the origin of high heat-producing granites becomes vital. Although beyond the scope of this paper, we will make some observations here which are pertinent to the definition of this problem. The geochemical characteristics of granitic magmas reflect the composition of the source rocks and petrogenetic processes, such as fractional crystallisation, which modify elemental concentrations in the melt. Nd isotopic studies of granites are particularly useful in discriminating between mantle and crustal sources of different ages (e.g. [43]). The Nd isotopic record of Archaean–Mesoproterozoic granites from the SAHFA displays a large range in initial $\varepsilon$Nd from 2.8 to $-11.1$, suggesting considerable variations in the proportion and isotopic composition of crust and juvenile mantle material within these rocks [35–39,44]. Of particular interest are the initial $\varepsilon$Nd values of high heat-producing granites of the Mount Painter Province, which are quite high and show very limited variation from $-3.2$ to $-0.5$. Extreme fractionation of melts containing only a small enriched crustal component is required to reconcile high $\varepsilon$Nd values with elevated U, Th and K concentrations.

## 6. Discussion

In the previous sections, we have shown that the high heat flow of the SAHFA is largely the result of elevated crustal heat production, with inferences about the seismic velocity of the upper mantle supporting the notion that mantle heat flow is less than 30 mW $m^{-2}$. This suggests that the crust in this region contributes on average 60–75 mW $m^{-2}$ to the surface heat flow, which is 2–3 times what would be expected on the basis of terranes of comparable or younger age in other continents. Such a high crustal radiogenic component implies that U, Th and K concentrations in the SAHFA are significantly higher than in typical crustal profiles, posing the question of how such elevated concentrations of heat-producing elements become localised in this crustal zone. Indeed, the concentrations amount to several times the crustal average and appear to require a source region of much greater volume than the directly underlying crust and mantle, especially given that lower crustal compositions are unlikely to represent a significant reservoir for radiogenic elements (e.g. [45]).

The extraordinary enrichment in heat-producing elements evident in the SAHFA suggests that the heat production character of the continental crust is rather more variable than indicated in recent reviews of heat production distributions (e.g. [3,5]). While exceptional, the SAHFA does not appear to be unique. For example, Lewis and Hyndman [46] have documented heat flow regimes from the northern Cordillera transect of Canada which are similar to the region described here. In this transect, heat flow increases from 40–60 mW $m^{-2}$ in the Archaean North American Craton to $\sim$90 mW $m^{-2}$ across the Hottah and Fort Simpson terranes, reaching $\sim$120 mW $m^{-2}$ in the Nahanni terrane. Although these heat flow values are consistent with elevated heat flow measurements further west in the Cordillera, inferences on upper mantle thermal regimes derived from seismic velocity determinations suggest that the exceptional heat flow in this region is due to elevated crustal heat production [46]. These occurrences suggest caution in the use of so-called 'global averages', at least until the heat flow dataset is extended to provide a more comprehensive coverage of regions outside North America and Europe.

We have shown that elevated crustal heat production values need not lead to excessive upper mantle temperatures provided that mantle heat flow is low and the heat production is mainly confined to the upper crust. However, an important consequence of this enrichment is that thermal regimes at depth are extremely sensitive to small changes in the vertical distribution of crustal heat production, for example due to burial beneath a sedimentary pile. For the parameters appropriate to the SAHFA and thermal conductivities of 2.5–3 W $m^{-1}$ $K^{-1}$, a change in heat production depth of 1 km produces a long-term increase in temperature of 20–30°C at any depth below the heat production. As outlined by Sandiford et al. [42], the sensitivity of crustal thermal regimes to the depth of the heat production distribution has important implications for the tectonic evolution of South Australia. By the earliest Phanerozoic, the high heat-producing Proterozoic basement of the SAHFA was differentially buried by virtue of the distribution of sedimentation associated with the development of the Adelaide Geosyncline. During periods of subsequent tectonic compression (during the Delamerian Orogeny and more recently in the last 5 Ma), deformation has been strongly localised where this basement was most deeply buried. This reflects a type of large scale basin inversion which is mechanically explicable in terms of the thermal consequences of differential burial of high heat-producing basement terranes [42].


## Acknowledgements

We thank Primary Industries of South Australia (PIRSA) for access to the South Australia Geoscientific GIS Dataset and Kathy Stewart for many useful discussions on the geochemistry of Proterozoic granites in South Australia. Hans Jurgen Förster, Simon Turner and Ross Taylor are thanked for helpful reviews.*[AH]*


## References


[1] I. Vitorello, H.N. Pollack, On the variation of continental heat flow with age and the thermal evolution of the continents, J. Geophys. Res. 85 (1980) 983–995.

[2] P. Morgan, The thermal structure and thermal evolution of the continental lithosphere, in: H.N. Pollack, V.R. Murthy (Eds.), Structure and Evolution of the Continental Lithosphere, Phys. Chem. Earth 15, 1984, pp. 107–193.

[3] R.L. Rudnick, W.F. McDonough, R.J. O'Connell, Thermal structure, thickness and composition of continental lithosphere, Chem. Geol. 145 (1998) 395–411.

[4] S.R. Taylor, S.M. McLennan, The Continental Crust: its Composition and Evolution, Blackwell Scientific Publications, Oxford, 1985, 312 pp.

[5] S.M. McLennan, S.R. Taylor, Heat flow and the chemical composition of continental crust, J. Geol. 104 (1996) 369–377.

[6] J.G. Sclater, C.J. Jaupart, D. Galson, The heat flow through oceanic and continental crust and the heat loss of the earth, Rev. Geophys. Space Phys. 18 (1980) 269–311.

[7] H.N. Pollack, S.J. Hurter, J.R. Johnson, Heat flow from the earth's interior: Analysis of the global data set, Rev. Geophys. 31 (1993) 267–280.

[8] A.A. Nyblade, H.N. Pollack, A global analysis of heat flow from Precambrian terranes: implications for the thermal structure of Archaean and Proterozoic lithosphere, J. Geophys. Res. 98 (1993) 12207–12218.

[9] M.T. McCulloch, Sm–Nd constraints on the evolution of Precambrian crust in the Australian continent, AGU Geodyn. Ser. 17 (1987) 115–130.

[10] L.O. Nicolayson, R.J. Hart, H.N. Gale, The Vredefort radioelement profile extended to supracrustal strata at Carletonville, with implications for continental heat flow, J. Geophys. Res. 86 (1981) 10653–10661.

[11] L.D. Ashwal, P. Morgan, S.A. Kelley, J.A. Percival, Heat production in an Archean crustal profile and implications for heat flow and mobilization of heat-producing elements, Earth Planet. Sci. Lett. 85 (1987) 439–450.

[12] D.M. Fountain, M.H. Salisbury, K.P. Furlong, Heat production and thermal conductivity of rocks from the Pikwitonei–Sachigo continental cross section, central Manitoba: implications for the thermal structure of Archean crust, Can. J. Earth Sci. 24 (1987) 1583–1594.

[13] C. Pinet, C. Jaupart, The vertical distribution of radiogenic heat production in the Precambrian crust of Norway and Sweden: geothermal implications, Geophys. Res. Lett. 14 (1987) 260–263.

[14] R.A. Ketcham, Distribution of heat-producing elements in the upper and middle crust of southern and west central Arizona: evidence from core complexes, J. Geophys. Res. 101 (1996) 13611–13632.

[15] P. Morgan, J.H. Sass, Thermal regime of the continental lithosphere, J. Geodyn. 1 (1984) 143–166.

[16] D.S. Chapman, K.P. Furlong, Continental heat flow–age relationships, EOS Trans. AGU 58 (1977) 1240.
[17] S. Ballard, H.N. Pollack, Diversion of heat by Archean cratons: a model for southern Africa, Earth Planet. Sci. Lett. 85 (1987) 253–264.
[18] J.H. Sass, A.H. Lachenbruch, Thermal regime of the Australian continental crust, in: M.W. McElhinny (Ed.), The Earth – its Origin, Structure and Evolution, Academic Press, London, 1979, pp. 301–351.
[19] J.F. Drexel, W.V. Preiss, A.J. Parker, The Geology of South Australia, Vol. I, The Precambrian, Geol. Surv. South Aust. Bull. 54, 1993, 242 pp.
[20] S.J. Daly, C.M. Fanning, M.C. Fairclough, Tectonic evolution and exploration potential of the Gawler Craton, South Australia, AGSO J. Aust. Geol. Geophys. 17 (1998) 145–168.
[21] P.M. Ashley, N.D.J. Cook, C.M. Fanning, Geochemistry and age of metamorphosed felsic igneous rocks with A-type affinities in the Willyama Supergroup, Olary Block, South Australia, and implications for mineral exploration, Lithos 38 (1996) 167–184.
[22] J.P. Cull, An appraisal of Australian heat flow data, BMR J. Aust. Geol. Geophys. 7 (1982) 11–21.
[23] G.A. Houseman, J.P. Cull, P.M. Muir, H.L. Paterson, Geothermal signatures and uranium ore deposits on the Stuart Shelf of South Australia, Geophysics 54 (1989) 158–170.
[24] J.H. Sass, J.C. Jaeger, R.J. Munroe, Heat flow and near surface radioactivity in the Australian continental crust, United States Geological Survey, open file report 76-250, 1976.
[25] L.E. Howard, J.H. Sass, Terrestrial heat flow in Australia, J. Geophys. Res. 69 (1964) 1617–1626.
[26] K. Gallagher, Some strategies for estimating present day heat flow from exploration wells, with examples, Exp. Geophys. 21 (1990) 145–159.
[27] C. Jaupart, J.C. Mareschal, The thermal structure and thickness of continental roots, Lithos 48 (1999) 93–114.
[28] V. Tokarev, M. Sandiford, V. Gostin, Landscape evolution in the Mount Lofty Ranges: implications for regolith development, in: G. Taylor, C. Pain (Eds.), Regolith '98: New Approaches to an Old Continent, 1999, pp. 131–139.
[29] B.W. Smith, J.R. Presscott, Thermoluminescence dating of Mount Schank, South Australia, Aust. J. Earth Sci. 34 (1987) 335–342.
[30] J.F. Drexel, W.V. Preiss, The Geology of South Australia, Vol. II, The Phanerozoic, Geol. Surv. South Aust. Bull. 54, 1995, 347 pp.
[31] J.P. Cull, D. Conley, Geothermal gradients and heat flow in Australian sedimentary basins, BMR J. Aust. Geol. Geophys. 8 (1983) 329–337.
[32] A. Zielhuis, R.D. van der Hilst, Upper-mantle shear velocity beneath eastern Australia from inversion of waveforms from Skippy portable arrays, Geophys. J. Int. 127 (1996) 1–16.
[33] M. Sandiford, S.N. McLaren, Thermo-mechanical controls on heat production distributions and the long-term evolution of the continents, in: M. Brown, T. Rushmer (Eds.), Evolution and Differentiation of the Continental Crust (submitted).
[34] F. Birch, R.F. Roy, E.R. Decker, Heat flow and thermal history in New England and New York, in: E.A. Zen, W.S. White, J.B. Hadley, J.B. Thompson (Eds.), Studies of Appalacian Geology, Northern and Maritime, Interscience, New York, 1968, pp. 437–452.
[35] South Australia Geoscientific GIS Dataset, CD ROM, Mines and Energy South Australia, 1997.
[36] R.A. Creaser, The geology and petrology of middle Proterozoic felsic magmatism of the Stuart Shelf, South Australia, Latrobe University Ph.D. thesis (unpublished), 1989.
[37] K. Stewart, High temperature felsic magmatism and the role of mantle magmas in Proterozoic crustal growth, the Gawler Range Volcanic province, University of Adelaide Ph.D. thesis (unpublished), 1992.
[38] P.M. Ashley, Sodic granitoids and felsic gneisses associated with uranium–thorium mineralisation, Crockers Well, South Australia, Min. Depos. 19 (1984) 23–30.
[39] B.F. Schaefer, Insights into Proterozoic tectonics from the southern Eyre Peninsula, South Australia, University of Adelaide Ph.D. thesis (unpublished), 1998.
[40] R. Haenel, L. Rybach, L. Stegena, Handbook of Terrestrial Heat-Flow Density Determination; with Guidelines and Recommendations of the International Heat Flow Commission, Kluwer academic publishers, Dordrecht, 1988, 486 pp.
[41] C.M.R. Fowler, The Solid Earth: An Introduction to Global Geophysics, Cambridge University, Cambridge, 1990, 472 pp.
[42] M. Sandiford, M. Hand, S.N. McLaren, High geothermal gradient metamorphism during thermal subsidence, Earth Planet. Sci. Lett. 163 (1998) 149–165.
[43] P.J. Patchett, Isotopic studies of Proterozoic crustal growth and evolution, in: K. Condie (Ed.), Proterozoic Crustal Evolution, Elsevier, 1992, pp. 481–508.
[44] S. Turner, J. Foden, M. Sandiford, D. Bruce, Sm–Nd evidence for the provenance of sediments from the Adelaide Fold Belt and southeastern Australia with implications for episodic crustal addition, Geochim. Cosmochim. Acta 57 (1993) 1837–1856.
[45] R. Rudnick, D. Fountain, Nature and composition of the continental crust: A lower crustal perspective, Rev. Geophys. 33 (1995) 267–309.
[46] T. Lewis, R. Hyndman, High heat flow along the SNORCLE transect, in: F. Cook, P. Erdmer (Eds.), Slave-Northern Cordillera Lithospheric Evolution (SNORCLE) Transect and Cordilleran Tectonics Workshop Meeting, Lithoprobe Report No. 69, University of Calgary, 1999, pp. 83–85.